Quantitative Carbon-13 Nuclear Magnetic Resonance Spectroscopic Study of Mobile Residues in Bacteriorhodopsin†

John L. Bowers and Eric Oldfield*
School of Chemical Sciences, University of Illinois at Urbana-Champaign, 505 South Mathews Avenue, Urbana, Illinois 61801
Received October 1, 1987; Revised Manuscript Received February 23, 1988

ABSTRACT: We have used quantitative carbon-13 nuclear magnetic resonance (NMR) spectroscopy to study the dynamic structure of the backbone of bacteriorhodopsin in the purple membrane of *Halobacterium halobium* R_1 and JW-3. NMR experiments were performed using an internal sucrose quantitation standard on purple membranes in which one of the following $^{13}C'$-labeled amino acids had been biosynthetically incorporated: glycine, isoleucine, leucine, lysine, phenylalanine, and valine. The results suggest that the C-terminus of the polypeptide chain backbone, and possibly one of the connecting loops, undergoes rapid, large angle fluctuations. Our results are compared with previous NMR and fluorescence spectroscopic data obtained on bacteriorhodopsin.

Bacteriorhodopsin (bR) is the only protein found in the photosynthetic purple membrane of *Halobacterium halobium*. It functions as an anaerobic light-driven proton pump, creating a pH gradient across the cell membrane which the cell utilizes to make ATP (Stoeckenius & Bogomolni, 1982). Both the static and dynamic structures of bR have been the subject of intense scrutiny, using a variety of physical techniques (Stoekenius et al., 1979; Henderson, 1977; Blaurock, 1982).

In our group, we have been interested in developing and applying nuclear magnetic resonance (NMR) techniques to determine the dynamic structure of bR, i.e., the rates and types of motions undergone by the various amino acid residues. Previous deuterium (^2H) NMR studies of side-chain-labeled amino acids in purple membranes concluded that surface regions of bR, or, more specifically, the C- and N-terminal tails and parts of the linking regions, were mobile on the deuterium NMR time scale (Keniry et al., 1984). This view is basically in accord with a recent fluorescence probe study (Marque et al., 1986) but is apparently at variance with an earlier fluorescence study (Renthal et al., 1983) and a series of observations by Lewis et al. (1985) and further results of R. G. Griffin and J. Herzfeld (Herzfeld et al., 1987). Because of these discrepancies, we have chosen to further investigate the question of the surface dynamics of bR, this time using a different nucleus, ^{13}C, combined with an absolute quantitation ("spin-counting") approach, which we believe should eliminate the possibilities of spectral distortion that may occur when using ^2H spin-echo methods. In this paper, we also extend our studies of motion in bR to include backbone motions. The basic experiment was as follows: First, a carbonyl carbon labeled amino acid was biosynthetically incorporated into bR. Second, quantitative high-resolution ^{13}C solution NMR spectra were acquired with a known amount of sucrose as an internal concentration standard, and the area of the (mobile) carbonyl resonance was compared to the peak areas of selected sucrose resonances. Third, gas chromatography/mass spectrometry of enriched bR was carried out in order to determine the exact enrichment in carbon-13. With this information, one can calculate the absolute number of mobile residues which give rise to the carbonyl carbon signal intensity. We have conducted these experiments on six different ^{13}C-labeled amino acids. The results indicate that the C-terminal backbone, and possibly one of the interconnecting loops, is in a highly disordered or mobile state. Our results are discussed in the context of our previous ^2H NMR studies, and the work of others (Renthal et al., 1983; Marque et al., 1986; Lewis et al., 1985; Herzfeld et al., 1987; Leo et al., 1987) on bR and on other membrane-bound proteins.

Materials and Methods

Purple Membrane Isolation and Purification. *Halobacterium halobium* strains R_1 and JW-3 were grown as previously described (Kinsey et al., 1981a) except $^{13}C'$-labeled amino acids were substituted for the normal nonlabeled amino acids. [1-^{13}C]Glycine (99%), L-[1-^{13}C]leucine (99%), and L-[1-^{13}C]lysine hydrochloride (90%) were purchased from Stohler/KOR isotopes (Cambridge, MA). L-[1-^{13}C]Isoleucine (99%), L-[1-^{13}C]phenylalanine (99%), and L-[1-^{13}C]valine (99%) were purchased from Tracer Technologies Inc. (Somerville, MA). L-[1-^{13}C]Valine (93%) was also obtained from the Stable Isotopes Resource of Los Alamos National Laboratory (Los Alamos, NM). Carbon-13-labeled amino acids were incorporated into defined media at the following concentrations: L-[1-^{13}C]Gly, 0.3 g/5 L; L-[1-^{13}C]Ile, 0.2 g/5 L; L-[1-^{13}C]Leu, 0.2 g/5 L; L-[1-^{13}C]Lys. 0.4 g/5 L; L-[1-^{13}C]Phe, 0.65 g/5 L; L-[1-^{13}C]Val, 1.5 g/5 L. Purple membranes were isolated essentially by the method of Becher and Cassim (1975) with minor modifications (Kinsey et al., 1981a,b). The stepwise sucrose gradient (45%, 40%, 38%, 36%, and 16% sucrose) was used on three samples after quantitative ^{13}C NMR had been run. Two of the three samples aggregated in 3 M KCl after the sucrose gradient. One sample, [$^{13}C'$]Val (strain R_1), did not aggregate in 3 M KCl after the sucrose gradient. Fractions F_1 and F_2 of the unaggregated [$^{13}C'$]Val samples were pooled (corresponding to purple membranes in the 40% and 38 wt % sucrose), and quantitative ^{13}C NMR was performed on them. Essentially identical NMR results were obtained, before and after the sucrose gradient, so this step was omitted in the rest of the samples, and red membrane content was monitored by using first-derivative ultraviolet/visible spectroscopy (UV/Vis) (vide infra).

Gel Electrophoresis. Sodium dodecyl sulfate-polyacrylamide gel electrophoresis (SDS-PAGE) was employed to monitor bR purity. In Figure 1, we show a 13% acrylamide

† This work was supported by National Science Foundation Grant DMB 84-16771.

0006-2960/88/0427-5156$01.50/0

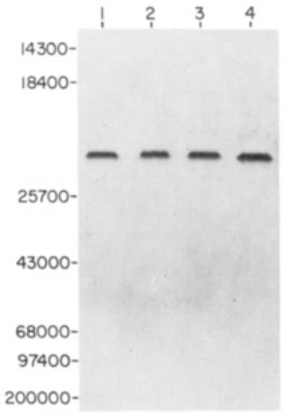

FIGURE 1: 13% acrylamide SDS–PAGE of four ^{13}C′-labeled bR preparations. Lane 1, [^{13}C′]valine-bR; lane 2, [^{13}C′]leucine-bR; lane 3, [^{13}C′]isoleucine-bR; lane 4, [^{13}C′]lysine-bR.

SDS–PAGE electrophoretogram of four different bR preparations, stained with Coomassie Brilliant Blue. Gel and sample conditions were as described by Laemmli (1970) except a 5% stacking gel was used. Intact bR runs anomalously under these conditions and had an apparent molecular weight of 21 000. Photodensitometry of these gels showed less than a 2% impurity was present in the bR samples. As an added check of protein homogeneity, protein was also visualized by using a silver stain, which is sensitive to the nanogram level, following the procedure of Wray et al. (1981). No extra bands were detected with a silver stain. Finally, gels were run under conditions optimized for small peptide fragments (Dumont et al., 1985). No added bands were detected under these conditions either.

The second purity check performed was the ratio of protein absorbance at 280 nm to chromophore absorbance at 568 nm. Literature values of this ratio, for purified purple membranes, range from 1.7 to 2.0 (Becher & Cassim, 1975; Oesterhelt & Stoeckenius, 1971). Our preparations were found to range from 1.8 to 1.9 and were determined with a Cary Model 219 UV/Vis spectrophotometer (Varian Associates, Palo Alto, CA).

Red Membrane Assay. It has been suggested (Herzfeld et al., 1987) that previous ^{2}H NMR results (Keniry et al., 1984) were due to red membrane contamination. Red membrane content of ^{13}C′-labeled purple membranes was therefore estimated by measurement of the residual absorption at 500 nm after bleaching with detergent (Lozier, 1982). Purple membranes were found to contain from 1% to 6% red membrane by this assay, the average value being 4%.

Carotenoid contamination was also assayed using the first derivative of the UV/Vis absorption spectrum of the bR samples. In Figure 2, we show the UV/Vis absorption and first-derivative spectra of red membranes (Figure 2A), purple membranes (Figure 2B), and a mixture of the two membranes (Figure 2C). Red membrane contamination of purple membrane samples causes shoulders in the absorption spectra of the purple membrane at 470, 498, and 533 nm. This is most easily seen in the first-derivative spectrum where the shoulders appear as peaks (Figure 2A,C). The heights of these peaks are directly proportional to the amount of red membrane in the sample. A calibration curve was made by titrating purple membrane with red membrane to a known concentration of red membrane and measuring and resultant height of only the largest peak in the first-derivative spectrum at 533 nm (distance *d* in Figure 2C). This curve was linear from 0% to 25% red membrane. Red membrane was grown and prepared according to the procedure of Oesterhelt and Stoeckenius

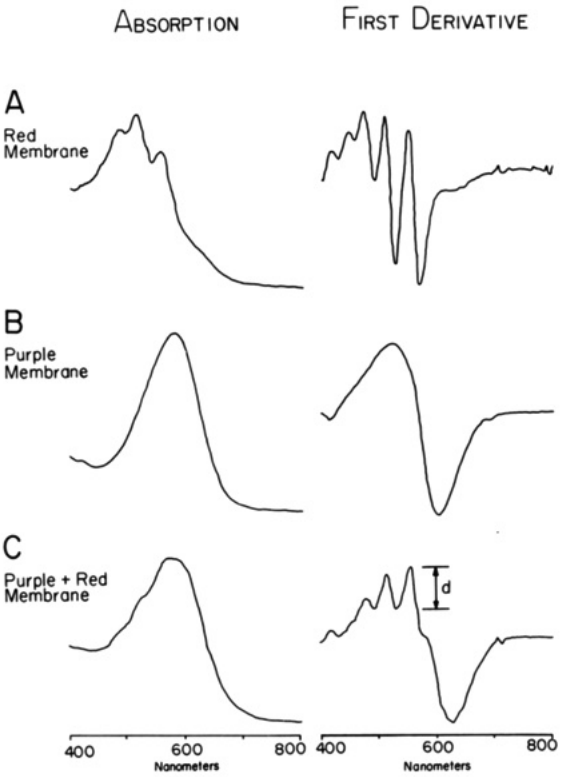

FIGURE 2: Absorption and first-derivative visible spectra (from 400 to 800 nm) of (A) red membranes, (B) purple membranes, and (C) red and purple membranes. The distance *d* is proportional to the amount of red membrane impurity in the purple membrane preparation, in this case 9% red membrane. All membranes were isolated from strain JW-3.

(1974), except the defined medium was substituted for bacteriological peptone media. Red membrane concentration was assayed according to the method of Lowry et al. (1951). First-derivative UV/Vis spectra were acquired on a Hewlett-Packard (Palo Alto, CA) Model 8451A diode array spectrophotometer. Purple membrane samples were found to contain between 0% and 3% red membrane, the average value being 2%, using this assay.

"3 M KCl Test". The last "quality control" test performed on the purple membranes was an "aggregation test" in 3 M KCl. Purple membranes were gently dispersed in 3 mL of 3 M KCl using a Pasteur pipet until a homogeneous, light purple solution ($A_{568} \approx 0.35$) was obtained. The solution was then left at room temperature in a stoppered test tube and checked for aggregation after 24 h. High-resolution ^{13}C solution NMR of samples that aggregated in 3 M KCl did not yield a narrow carbonyl resonance, while samples which remained homogeneous did (data not shown). SDS–PAGE of samples that aggregated in 3 M KCl, and those that did not, showed no discernible difference; i.e., there was no evidence of proteolysis. Although we have no explanation at this time for the empirical correlation between aggregation in 3 M KCl and high-resolution NMR signals, the KCl test appears to be a sensitive indicator of the state of the membrane surface, or at least a predictor of NMR behavior.

Sample Preparation. Purple membrane pellets were diluted by the addition of 2.4–3.0 mL of 50 mM Na_2HPO_4, pH 7.0, and mixed until homogeneous. The concentration of bR was determined after dilution of 100 μL of purple membrane solution to 25 mL with phosphate buffer. The absorbance at 568 nm was measured on a Cary Model 219 UV/Vis spectrophotometer, and the concentration was determined on the basis of a molar absorptivity of 63 000 cm^{-1} mol^{-1} L. Con-

centrations of bR ranged from 17 to 35 mg mL^{-1}. A known amount of sucrose, for use as an internal concentration standard, was then weighed into a 2-mL volumetric flask and the purple membrane solution added to the mark. Typically, about 35 mg of sucrose was used.

NMR Spectroscopy. ^{13}C NMR spectra were obtained on a "home-built" NMR spectrometer, which consists of a 2.0-in. bore 11.7-T superconducting solenoid (Oxford Instruments, Osney Mead, Oxford, U.K.) with a Nicolet (Madison, WI) 1280 computer, an Amplifer Research (Souderton, PA) Model 200-L radio-frequency amplifier, and either a 5-mm or a 10-mm solution NMR probe (Cryomagnet Systems, Indianapolis, IN). Field-lock was maintained by using a small, concentric, capillary tube of D_2O, inside the sample tube. All spectra were referenced to an external standard of dioxane (δ 67.86 ppm from tetramethylsilane). High-frequency, low-field, deshielded, paramagnetic shifts are denoted as positive (IUPAC δ scale).

Special care was taken to ensure quantitative NMR measurements. Acquisition parameters were the following: spectral width of ±15 kHz, filter bandwidth of ±20 kHz, 16K data points, acquisition time of 270 ms, preacquisition delay of 66 μs, ~14 000 acquisitions, and a recycle delay of 12 s. All spectra were acquired without proton decoupling using single 90° pulse excitation, and allowing a minimum of $5T_1$ between pulses, so that at least 99% of the magnetization had relaxed to its equilibrium value (Gillet & Delpuech, 1980). Spin–lattice relaxation times (T_1) were measured by using the inversion–recovery pulse sequence with a composite 180° pulse (90_x–180_y–90_x) (Freeman et al., 1980). The T_1 values for the $^{13}C'$ amino acid labeled purple membranes were the following: Leu, 0.9 s; Gly, 1.0 s; Lys, 1.1 s; Ile, 1.4 s; Val, 1.5 s; and Phe, 1.9 s. T_1's for the sucrose resonances used in quantitation were the following: C2′, 2.5 s; C1, 0.5 s.

Carbon-13 90° pulse widths were 18–20 μs for the 10-mm probe and 13 μs for the 5-mm probe, using 60 W of radio-frequency power. The spectral window of interest is 100 ppm, or at 11.7 T 12.5 kHz. Data acquisition in quadrature effectively reduces this by a factor of 2 to 6.25 kHz. A pulse width of 20 μs is short enough to uniformly excite this spectral width (Martin et al., 1980). We verified this experimentally in two ways. First, we measured the ^{13}C signal intensity for the triplet of [$^2H_6$]benzene, as a function of offset from resonance, using a filter bandwidth of ±20 kHz. Significant signal attenuation did not occur until an offset of 8.5 kHz, at which point spectral intensity drops off very quickly, due to both pulse power falloff and filter attenuation (Thiault & Mersseman, 1975). Second, we obtained identical quantitative NMR results on a sample run in a 10-mm probe with a 20-μs 90° pulse, and a 5-mm probe with 13-μs 90° pulse. Coupled spectra were acquired in all cases to avoid any intensity distortions due to a differential nuclear Overhauser effect (NOE).

Gas Chromatography/Mass Spectrometry. Gas chromatography/mass spectrometry (GC/MS) was performed on all samples to determine the level of ^{13}C enrichment. Purple membranes were lyophilized and then delipidated by extracting 3 times with chloroform/methanol (1:2 v/v). Delipidated membranes were hydrolyzed in vacuo in 6 N HCl at 110 °C for 24 h. Amino acids were derivatized to their *N*-trifluoroacetyl *n*-butyl esters following the procedure of White and Rudolph (1978). Capillary gas chromatography was performed on a Varian Model 3700 gas chromatograph (Palo Alto, CA) using a J&W DB-5 fused silica capillary column (Rancho Cordera, CA). Electron-impact mass spectrometry was performed on a VG Instruments (Manchester, England) Model 705E mass spectrometer, and the atom percent carbon-13 was calculated according to Campbell (1974).

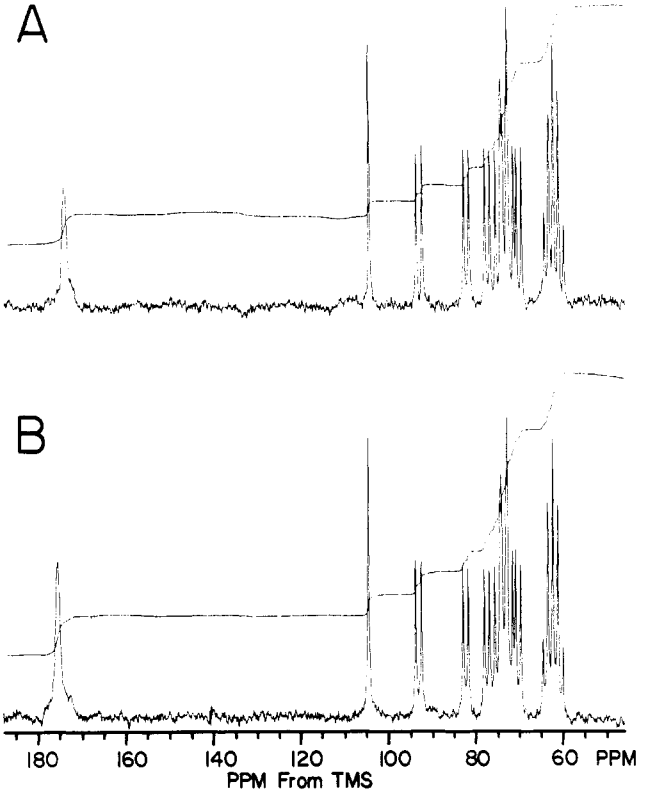

FIGURE 3: Proton-coupled 125-MHz solution carbon-13 Fourier-transform NMR spectra of (A) [$^{13}C'$]valine-labeled bR and sucrose (recycle time 12 s, 20-μs 90° pulse excitation) and (B) [$^{13}C'$]-leucine-labeled bR and sucrose (recycle time 12 s, 18-μs 90° pulse excitation).

Results and Discussion

We show in Figure 3 the 125.7-MHz proton-coupled carbon-13 solution NMR spectra, and corresponding integrals, of [$^{13}C'$]valine-labeled bR (strain JW-3) and sucrose (Figure 3A) and [$^{13}C'$]leucine-labeled bR (strain JW-3) and sucrose (Figure 3B). The high-frequency carbonyl resonances at ~175 ppm have widths at half-height of 150 and 125 Hz, respectively, while the sucrose resonances to lower frequency have about 15-Hz line widths. The integrals used for quantitation were the carbonyl integral and the average of the integrals of the anomeric carbon (C2′) of sucrose, at 104.6 ppm, and the protonated carbon (C1) integral, at 90 ppm. The integrals were corrected for differential T_2 effects during the preacquisition delay and for the carbonyl natural-abundance background signal.

Our results indicate that the origin of the carbonyl signal is from surface residues, and not from red membrane contamination as has been suggested for previous ^2H NMR studies of bR (Keniry et al., 1984) by Herzfeld et al. (1987). Omission of the sucrose gradient, as previously noted, in the Becher and Cassim preparation did not affect our quantitative NMR results, as we obtained essentially identical quantitation before and after the sucrose gradient. In addition, quantitative NMR of a glycine-labeled red membrane sample of known concentration revealed that the sample of glycine-labeled purple membranes would have had to be 21% red membrane to yield a signal of the same intensity as observed in the purple membrane spectrum. We believe, on the basis of the results discussed above, that we are far below this level, by our best experimental estimates in the 0–3% range. Also, as shown in Figure 4, we have obtained NMR spectra of the same label

Table I: Comparison between ^{2}H and Quantitative ^{13}C NMR Data on Labeled bR and Predictions of Model Building[a]

amino acid	no. of residues	% surface residues[c]		% C-terminus[a]		no. of residues in[c] C-terminus	
		model	^{2}H NMR[d]	model	^{13}C NMR[e]	model	^{13}C NMR[c]
Gly	25	32	32 ± 2	12	14	3	3.5
Val[f]	21	29	35 ± 2	0	7[g]	0[f]	1.45
Leu	36	6	10 ± 2	3	4[h]	1	1.4
Ile	15	13	15 ± 4	7	6	1	0.85
Lys	7	29	25 ± 4	0	0	0	−0.1
Phe	13	23	11 ± 4[i]	8	7	1	0.95

[a] Engelman et al. (1982) model used, as described previously (Keniry et al., 1984; Bowers et al., 1986). [b] Total number of residues of a specific type in bR. [c] Calculated as described in Keniry et al. (1984), from Engelman et al. (1982) model. [d] From Bowers et al. (1986). [e] Percent of residues of a given type in the C-terminus, from Engelman et al. (1982) model. Corrected for natural-abundance contribution and differential T_2 effects. [f] No residue of this type in C-terminus; see text for details. [g] Average of four determinations. [h] Average of two determinations. [i] Low value presumably due to echo distortion phenomenon.

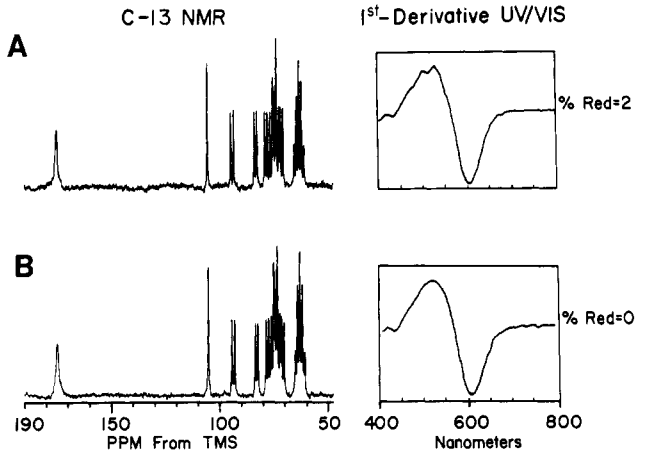

FIGURE 4: Proton-coupled 125-MHz solution carbon-13 Fourier-transform NMR spectra and first-derivative UV/Vis spectra of two different samples of [^{13}C']valine-labeled bR. (A) Quantitative NMR yields 1.4 residues; UV/Vis yields 2% red membrane. (B) Quantitative NMR yields 1.3 residues; UV/Vis yields 0% red membrane.

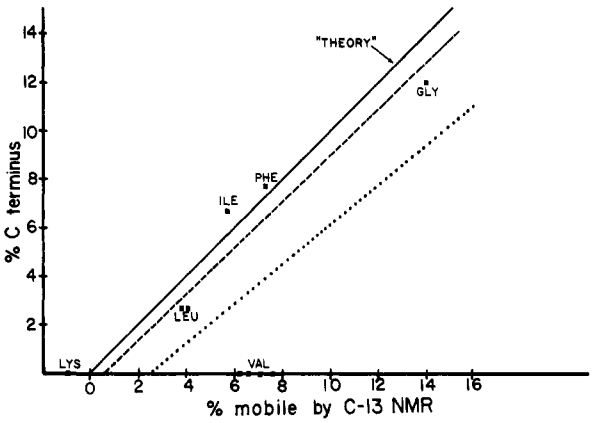

FIGURE 5: Correlation between percent of residues of a given type in the C-terminus of bR [Engelman (1982) model] to the percent mobile residues observed by carbon-13 NMR. The solid line represents a 1:1 correlation ($y = x$). The dotted line represents the least-squares fit including valine ($y = 0.80x - 1.91$). The dashed line represents the least-squares fit excluding valine ($y = 0.95x - 0.38$).

(Val-C', strain R_1) with differing amounts of red membrane by first-derivative UV/Vis, which yield essentially the same result by ^{13}C NMR. For example, the sample in Figure 4A contains 2% red membrane (by UV/Vis), while that of Figure 4B contains 0%. However, the results of quantitative ^{13}C NMR reveal essentially identical C' intensities.

Comparisons with Previous NMR Results. We show in Table I the full compilation of our quantitative ^{13}C NMR results together with, for purposes of comparison, the previous results obtained via ^{2}H NMR (Keniry et al., 1984; Bowers et al., 1986). There are clearly major differences between the two data sets which need to be accounted for. In particular, the ^{2}H NMR results indicate more mobile "surface" residues than do our current ^{13}C NMR results. There are at least three possible reasons for these differences. *First*, our previous studies could have been compromised by red membrane contamination. However, essentially identical protocols have been used in the present work, which has excluded significant red membrane contamination, as discussed in some detail previously. *Second*, our previous ^{2}H NMR studies could have been compromised by quadrupole echo distortion phenomena. Since we did not do absolute quantitations in that study, this possibility cannot be ruled out. However, with the possible exception of Phe and Tyr, we believe this is unlikely, since most residues monitored were mobile methyl groups. *Third*, the ^{13}C and ^{2}H NMR results may in fact be totally consistent, and may simply reflect the fact that in each of the ^{13}C labeling experiments we have used a ^{13}C' *backbone*-labeled amino acid, while in the ^{2}H NMR study, *side chains* were labeled. Thus, we believe it is quite likely that ^{13}C NMR is only monitoring those residues which are *extremely* mobile, and which are located primarily in the C-terminus. This type of phenomenon has been discussed by Colnago et al. (1987), who studied the dynamics of fd coat protein in bacteriophage, and Leo et al. (1987), who studied the dynamics of fd coat protein in lipid bilayers. In both studies, it was found that "many of the side-chains of residues with immobile backbone sites undergo large amplitude jump motions." These workers also found mobile C- and N-terminal signals in the fd coat protein.

We thus believe that all of our results obtained so far can be adequately accounted for by a model in which the C-terminus of bR is highly mobile, while the loops are less so. Thus, backbone motion in the loops is inadequate to give the narrow (~100 Hz) lines observed in the typical "high-resolution" ^{13}C NMR spectrum (from the C-terminus), but side-chain motion in the loops, about multiple bonds, is more than adequate to cause motional narrowing of the ^{2}H NMR resonance to the ~1–2-kHz values found previously (Keniry et al., 1984).

We thus show in Figure 5 a graphical summary of our current ^{13}C NMR results in which we have plotted the percent of residues in the C-terminus *versus* the percent of mobile residues, as determined by quantitative ^{13}C NMR spectroscopy. The solid line represents the equation $y = x$, which would pertain for a 1 to 1 correlation between the percent of residues in the C-terminus and the percent of mobile residues found by ^{13}C NMR. If the value for valine is included, there is a poor correlation (dotted line, Figure 5, correlation coefficient = 0.64). There are no valine residues in the C-terminus, and yet four determinations on three different preparations of [^{13}C']valine-labeled bR yielded essentially the same result,

1.4 residues. This could indicate some mobility in other regions of the protein. The loop Val-167 is in is the largest loop, being comprised of ~19 amino acids, with Val-167 near the middle, furthest away from the membrane surface. This is a prime candidate for a mobile valine, although we cannot rule out other possibilities.

A vastly improved correlation (dashed line, Figure 5, correlation coefficient = 0.96) is obtained if the valine point is eliminated, for the reasons given above. We now find that there is an excellent aggreement between the percent residues in the C-terminus and the percent residues found to be mobile by quantitative ^{13}C NMR. We believe these results, based on absolute quantitation with five different labeled amino acids, strongly support the idea that the C-terminus of bacteriorhodopsin is highly mobile in native, unaggregated, purple membrane samples.

In a recent paper of Herzfeld et al. (1987), they describe their qualitative ^2H NMR spectra of leucine-d_3-labeled bR (strain JW-3). They conclude that few, if any, of the surface residues in bacteriorhodopsin are moving isotropically on the ^2H NMR time scale and that the isotropic (^2H NMR) signal varies according to the degree of residual contamination of the sample with red membrane. We will comment briefly on their results: (1) There was no absolute quantitation of the ^2H NMR results presented, unlike in the present study. (2) There was no quantitation of the amount of red membrane present, unlike in the present study. (3) Their experimental digital resolution apparently represents approximately one to three points per peak (for the narrow line), confounding any reliable estimate of peak area, or even height [see Keniry et al. (1984), Figure 1K,M]. (4) Herzfeld et al. state that "the loss of the isotropic signal on proteolysis is best explained by preferential degradation of the contaminating protein ... the contaminants that we have observed are probably on the periphery of the membrane proteins ... and ... the contaminant is probably more vulnerable to proteolysis than is bacteriorhodopsin. ... It is not necessary to suppose that there is any aggregation-linked immobilization of residues in proteolysed samples". The facts are, however, that gels of proteolyzed samples show proteolysis, visual inspection shows the samples aggregate, and ^2H and ^{13}C NMR shows the isotropic peak disappears.

Comparison with Previous Fluorescence Results. As with the NMR results, there appear to be two schools of thought with regard to the interpretation of surface dynamics of bR in purple membrane. Renthal et al. (1983) conclude that "the labeled region of the C-terminal tail of bacteriorhodopsin is rigidly held at the membrane surface", while Marque et al. (1986), using a more hydrophilic probe, basically conclude the opposite. Our results are in agreement with the conclusions of the latter workers. It is difficult, however, to make a quantitative comparison with the fluorescence results since widely different time scales are involved, and since the fluorescence probe may cause local structural changes. Cross-linking reagents may also affect surface structure as viewed by NMR (Bowers et al., 1986).

Conclusions. The results we have presented in this publication represent, we believe, the first study of the structure of an intact biological membrane using absolute quantitative NMR techniques. We have incorporated six different backbone (C′) ^{13}C-labeled amino acids into the purple membrane of *H. halobium* and, using absolute spin-counting techniques, have determined the percent of residues which are highly mobile. We find using lysine, leucine, isoleucine, phenylalanine, and glycine that an excellent correlation (correlation coefficient = 0.96) is found between the percent residues in the C-terminus and the percent of residues of a given type which are mobile by ^{13}C NMR. This strongly suggests that the C-terminus is highly mobile, at least under our solution conditions, in agreement with the electron diffraction results of Wallace and Henderson (1982) and recent fluorescence results of Marque et al. (1986), but in apparent disagreement with the earlier fluorescence conclusions of Renthal et al. (1983) and the NMR conclusions of Lewis et al. (1985) and Herzfeld et al. (1987). We believe that the presence of red membrane contamination cannot be a significant contributor to the observed narrow resonance, since in general the levels are much too low (0–3%) to account for the results observed. Also, the generally excellent agreement between the intensity expected and the intensity observed strongly argues against any artifactual origin of the narrow spectral features. Our results are also not inconsistent with our earlier ^2H NMR studies (Keniry et al., 1984; Bowers et al., 1986) since side chain, rather than backbone, labeled amino acids were used in the earlier studies, and Colnago et al. (1987) and Leo et al. (1987) have demonstrated, in other protein or protein–lipid systems, the occurrence of "mobile" side chains due to multiple internal rotations and librations, while backbone residues may be effectively "rigid". We thus believe that residues in the helical ("matrix") regions of bacteriorhodopsin in the purple membrane of *H. halobium* are rigid, while the surface regions are more mobile, with the C-terminus being extremely mobile, much as in a disordered random coil protein in solution, at least at the concentration levels and under the solution conditions we have employed.

ACKNOWLEDGMENTS

We thank Professors W. Stoeckenius and J. Herzfeld for providing the *H. halobium* strains R_1 and JW-3, R. G. Griffin and J. Herzfeld for stimulating discussion, Kathleen Hall for guidance and assistance in the GC/MS, and Gail Newton and Kimberly Carter for assistance with gel electrophoresis and Lowry determinations. We also thank the Stable Isotope Resource of Los Alamos National Laboratory (supported in part by NIH Grant RR-02231) for providing the L-[1-^{13}C]-valine.

REFERENCES

Becher, B. M., & Cassim, J. Y. (1975) *Prep. Biochem. 5*, 161–178.

Blaurock, A. E. (1982) *Methods Enzymol. 88*, 124–132.

Bowers, J. L., Smith, R. L., Coretsopoulos, C., Kunwar, A. C., Keniry, M., Shan, X., Gutowsky, H. S., & Oldfield, E. (1986) in *Progress in Protein–Lipid Interactions* (Watts, A., & Depont, J. J. H. H. M., Eds.) Vol. 2, pp 83–101, Elsevier Science Publishers B. V., Amsterdam, The Netherlands.

Campbell, I. M. (1974) *Bioorg. Chem. 3*, 386–397.

Colnago, L. A., Valentine, K. G., & Opella, S. J. (1987) *Biochemistry 26*, 847–854.

Dumont, M. E., Trewhella, J., Engelman, D. M., & Richards, F. M. (1985) *J. Membr. Biol. 88*, 233–247.

Engelman, D. M., Goldman, A., & Steitz, T. A. (1982) *Methods Enzymol. 88*, 81–88.

Freeman, R., Kempsell, S. P., & Levitt, M. H. (1980) *J. Magn. Reson. 38*, 453–479.

Gillet, S., & Delpuech, J.-J. (1980) *J. Magn. Reson. 38*, 433–445.

Henderson, R. (1977) *Annu. Rev. Biophys. Bioeng. 6*, 87–109.

Herzfeld, J., Mulliken, C. M., Siminovitch, D. J., & Griffin, R. G. (1987) *Biophys. J. 52*, 855–858.

Keniry, M. A., Gutowsky, H. S., & Oldfield, E. (1984) *Nature (London) 307*, 383–386.
Kinsey, R. A., Kintanar, A., & Oldfield, E. (1981a) *J. Biol. Chem. 256*, 9028–9036.
Kinsey, R. A., Kintanar, A., Tsai, M.-D., Smith, R. L., Janes, N., & Oldfield, E. (1981b) *J. Biol. Chem. 256*, 4146–4149.
Laemmli, U. K. (1970) *Nature (London) 227*, 680–685.
Leo, G. C., Colnago, L. A., Valentine, K. G., & Opella, S. J. (1987) *Biochemistry 26*, 854–862.
Lewis, B. A., Harbison, G. S., Herzfeld, J., & Griffin, R. G. (1985) *Biochemistry 24*, 4671–4679.
Lowry, O. H., Rosebrough, N. J., Farr, A. L., & Randall, R. J. (1951) *J. Biol. Chem. 193*, 265–275.
Lozier, R. H. (1982) *Methods Enzymol. 88*, 133–162.
Marque, J., Kinosita, K., Govindjee, R., Ikegami, A., Ebrey, T. G., & Otomo, J. (1986) *Biochemistry 25*, 5555–5559.
Martin, M. L., Delpuech, J.-J., & Martin, G. J. (1980) *Practical NMR Spectroscopy*, Heyden, London.
Oesterhelt, D., & Stoeckenius, W. (1971) *Nature (London), New Biol. 233*, 149–152.
Oesterhelt, D., & Stoeckenius, W. (1974) *Methods Enzymol. 31A*, 667–678.
Renthal, R., Dawson, N., Tuley, J., & Horowitz, P. (1983) *Biochemistry 22*, 5–12.
Stoeckenius, W., & Bogomolni, R. A. (1982) *Annu. Rev. Biochem. 52*, 587–616.
Stoeckenius, W., Lozier, R. H., & Bogomolni, R. A. (1979) *Biochim. Biophys. Acta 505*, 215–278.
Thiault, B., & Mersseman, M. (1975) *Org. Magn. Reson. 7*, 575–578.
Wallace, B. A., & Henderson, R. (1982) *Biophys. J. 39*, 233–239.
White, R. H., & Rudolph, F. B. (1978) *Biochim. Biophys. Acta 542*, 340–347.
Wray, W., Boulikas, T., Wray, V. P., & Hancock, R. (1981) *Anal. Biochem. 118*, 197–203.

Line-Shape Analysis of NMR Difference Spectra of an Anti-Spin-Label Antibody†

Tom Frey,‡ Jacob Anglister,§ and Harden M. McConnell*,‡
Stauffer Laboratory for Physical Chemistry, Stanford University, Stanford, California 94305, and Polymer Department, The Weizmann Institute of Science, Rehovot 76100, Israel

Received October 14, 1987; Revised Manuscript Received March 14, 1988

ABSTRACT: Specifically deuteriated Fab fragments of the anti-spin-label antibody AN02 were prepared. NMR difference spectra were obtained, in which the spectrum of Fab with some fraction of the binding sites occupied with spin-label hapten was subtracted from the spectrum of Fab with no spin-label. The peak heights were analyzed as a function of the fractional occupation of the binding site, using a computer program that calculates a best fit to the observed spectra. This method treats all of the peaks in the spectra simultaneously. Analyzing all peaks at once allows for the interdependencies in the spectra arising from overlap of positive and negative signals from different peaks. The fitting program calculates line widths for the peaks arising from protons in the binding site region. Almost all of the line widths calculated for the spectrum of the Fab complex with diamagnetic hapten dinitrophenyldiglycine were found to be narrower than the line widths of the corresponding resonances in the spectrum of Fab with an empty binding site. The distances of the binding site region protons from the unpaired electron of the hapten were also obtained from this calculation. Two tyrosine protons were found to be close (<7 Å) to this electron. These line-width and distance results are discussed with respect to the structure and dynamics of the antibody binding site.

In an effort to improve the understanding of antibody binding site structure, we have pursued an NMR study of the anti-spin-label antibody AN02. In previous work, we used biosynthetic deuteriation and protein chemistry with NMR to obtain information about the amino acid makeup of the binding site region (Anglister et al., 1984a; Frey et al., 1984) and to assign resonances to the heavy and light chains (Anglister et al., 1985). Nuclear magnetization transfer was used to identify the resonances of protons in close proximity to the hapten (Anglister et al., 1987). The effect of the paramagnetic hapten on the protein NMR spectrum was used to measure the distance of certain antibody protons from the unpaired electron of the hapten (Anglister et al., 1984b).

The effect of the hapten on the ANO2 resonance spectrum was described, and a technique for extracting distance information was discussed. This technique involves titrating the binding site of the Fab with paramagnetic hapten and subtracting the NMR spectrum taken at each titration point from the spectrum of the Fab with no hapten bound. The change in peak height of each resonance was analyzed as a function of fractional occupation of the binding site. Several tyrosine resonances displayed the theoretically expected behavior.

The technique presented in our earlier paper analyzed one signal at a time, required that the line width of the proton resonance be known, and assumed that the resonance signals were homogeneous and Lorentzian. Of course, this is not satisfactory for spectra with multiple, overlapping resonances. Further difficulties arise with line-width determination when resonances are very broad or very narrow, due to low signal to noise and digitization, respectively. In the present work, we find that simulation and computer fitting of the observed spectra can be used successfully to extract the desired line-width and distance information.

Materials and Methods

The preparation and purification of the AN02 antibody have been described. Fab fragments were prepared and purified as previously described. The affinity of AN02 for spin-label

† This work was supported by ONR Contract N00014-86-K-0388.
‡ Stanford University.
§ The Weizmann Institute of Science.

0006-2960/88/0427-5161$01.50/0